Mechatronics, Electrical Power, and Vehicular Technology 05 (2014) 67-74

Mechatronics, Electrical Power, and Vehicular Technology

e-ISSN:2088-6985
p-ISSN: 2087-3379
Accreditation Number: 432/Akred-LIPI/P2MI-LIPI/04/2012

www.mevjournal.com

PROPORTIONAL DERIVATIVE ACTIVE FORCE CONTROL FOR "X" CONFIGURATION QUADCOPTER

Ni'am Tamami [a],*, Endra Pitowarno [a], I Gede Puja Astawa [a]

[a] Electronics Engineering Polytechnic Institute of Surabaya
Kampus PENS, Jalan Raya ITS, Sukolilo, Surabaya 60111, Indonesia

Received 21 August 2014; received in revised form 10 September 2014; accepted 16 September 2014
Published online 24 December 2014

Abstract

This paper presents a stabilization control method for "x" configuration quadcopter using PDAFC (Proportional Derivative Active Force Control). PD is used to stabilize quadcopter, whereas AFC is used to reject disturbance uncertainty (e.g. wind) by estimating disturbance torque value of quadcopter. Simulation result shows that PDAFC is better than PD and AFC can minimize disturbance uncertainly effect. The sensitivity toward disturbance uncertainly can be set from sensitivity constant to get best performance of disturbance rejection. Constant disturbance simulation result shows that the best sensitivity constant (C_{sens}) is 0.15, the quadcopter maximum error is 0.125 radian and can stable in 5 seconds. Fluctuated disturbance simulation result shows that PDAFC with 0.18 sensitivity constant gives lowest RMS error value, there are 0.074 radian for sine disturbance, 0.055 radian for sawtooth disturbance, and 0.092 radian for square pulse disturbance.

Keywords: "x" configuration quadcopter, PD, AFC.

I. INTRODUCTION

Unmanned aerial vehicles (UAVs) have been developed and used over the last few years. UAVs can be built not only for a hobby but also for performing important task such as area mapping, surveillance, disaster monitoring, air pollution monitoring, etc. They are capable to hover without an on-board pilot. UAVs become good choice because it has low operational cost and also is safe in important task where risk to pilot are high.

Quadcopter has a simple structure. It utilises rotors which are directed upwards and placed at the end of a crossed frame. It is controlled by adjusting the angular velocities of each rotors. The quadcopter biggest advantage is that the blades do not have to be movable. A normal helicopter has blades that can be tilted up or down to vary lift. They have complex joints at the hub of the blade, which makes the blades hard to manufacture, difficult to maintain, and very dangerous if any failure occurs. Moreover, quadcopter can take off, land in limited spaces and hover above targets. These vehicles have certain advantages over conventional fixed-wing aircraft for surveillance and inspection tasks.

There are many researches about quadcopter control algorithm and uncertainty disturbance rejection. Bouabdallah et al. designed an LQ controller and PID controller then compared it [1]. The PID controller result is better than LQ controller. Jun Li and Yuntang Li designed PID controller to control angular and linear position, and succeeded to stabilize quadcopter [2]. Mokhtari and Benallegue applied state parameter control to quadcopter rotation angle [3]. By using state observer, quadcopter can measure external disturbance. Gupte et al. described that "x" configuration quadcopter is more stable than "+" configuration quadcopter because of the distribution of rotor force during hover [4]. Bora and Erdinc have been controlling position of quadcopter using PD controller and combined by using a vision system [5]. Pounds et al. developed independent linear SISO controllers to regulate quadcopter using PID controller [6]. A. Tayebi et al. proposed a controller which is based upon the compensation of the Coriolis and gyroscopic torques and the use of PD^2 feedback structure [7]. Sumantri et al. designed a sliding

* Corresponding Author. Tel: +6285733316323
E-mail: niam@eepis-its.edu

doi: 10.14203/j.mev.2014.v5.67-74

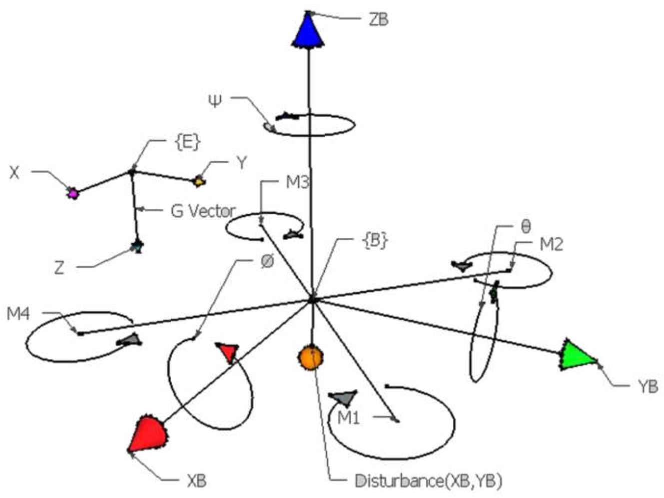

Figure 1. An “x” configuration quadcopter

mode control using a nonlinear sliding surface (NSS) to design a robust tracking controller for a quad-rotor helicopter [8]. Chen and Huzmezan used linear H∞ controller to achieve stabilization in angular rates, vertical velocity, longitudinal velocity, lateral velocity, yaw angle, and height of a quadcopter [9]. A linear H∞ controller can be designed to obtain stabilization and tracking performance using a systematical approach [10].

Pitowarno had designed Active Force Control and Knowledge-Based System for planar two-joint robot arm to improve performance of Active Force Control [11]. Katsura et al. have been modeled force sensing using disturbance observer without force sensor [12]. Chen et al. designed disturbance observer control for nonlinear system to control robotic manipulator [13].

It is very important to make a simple control algorithm to control the quadcopter stability although get uncertainty disturbance from environment. Because in real system, control algorithm will be embed in low speed data processing unit. PD can stabilize quadcopter but still not enough to maintain the quadcopter against uncertainty disturbance such as wind. AFC has the ability to estimate the force on the system without using complicated mathematical computation.

The purpose of this work is modelling and combining PD and AFC to control “x” configuration quadcopter when hover even if get uncertainty disturbance. This paper is structured as follows. Section 2, presents a quadcopter dynamic modelling. Section 3, deals quadcopter controller design. Section 4, presents the performance of the controller is shown in numerical simulations. Finally, in Section 5 conclusions of this work.

II. Quadcopter Modelling

Before designing the controller, in this section the mathematical model of the quadcopter will be presented. This dynamic model as much as possible same as the real quadcopter. It is contain the model of the rotor force and torque, gyroscopic effect, and the derived force model of “x” configuration quadcopter.

Figure 1 is the design of “x” configuration quadcopter. The rotors (M1, M2, M3, M4) are placed in sequence π/4, 3π/4, 5π/4, 7π/4. Two diagonal rotors (M1 and M3) are rotating in the same direction (counter clockwise) whereas the others (M2 and M4) in the clockwise direction to eliminate the anti-torque that caused by rotor rotation.

Absolute position of the quadcopter can be described by a coordinate position of the body frame {B} with reference earth frame {E}. Absolute attitude of the quadcopter can be described by three Euler’s angles (ϕ, θ, ψ),which are roll, pitch, and yaw with reference to body frame {B} when XB, YB, and ZB axis are in parallel with X, Y, and is rotated 180° Z axis.

To make a movement along XB axis, quadcopter must produce pitch torque (τ_y). It means, quadcopter decreases rotor speed at M1 and M4, and increases rotor speed at M2 and M3. Likewise to make movement along YB axis quadcopter must produce roll torque (τ_x). Quadcopter decreases rotor speed at M1 and M2, and increases rotor speed at M3 and M4. Then, to change quadcopter heading, quadcopter must produce yaw torque (τ_z) by increasing M1 and M3 rotor speed, and decreasing M2 and M4 rotor speed.

Figure 2 shows the force distribution in quadcopter. “F1, F2, F3, F4” arrows are thrust force of each motor, and "m.g" arrow is weight force of quadrotor. From Li et al., the thrust and hub force for each rotor (F_i, H_i) can be represented in equation (1) and (2) [2]. Thrust force is the resultant of the vertical forces acting on all blade elements. Hub force is the resultant of the horizontal forces acting on all blade elements.

$$F_i = \frac{1}{2}\rho C_T {\Omega_i}^2 = k_t {\Omega_i}^2 \quad (1)$$

$$H_i = \rho C_d {\Omega_i}^2 = \frac{2C_d}{C_T} F_i = K_d F_i = K_d \frac{1}{2}\rho C_T {\Omega_i}^2 = k_d {\Omega_i}^2 \quad (2)$$

where ρ is air density; C_T is thrust constant that depends on polar lift slope, geometric blade, velocity through motor, the ratio of the surface area and rotor disk area [6]. C_d is drag constant, and Ω_i is propeller rotation speed.

Quadcopter can change its position by combining translation and rotation angle. Linear movement on the quadcopter can be produced by total thrust force of the four rotors in equation (3), whereas changes in the angle of rotation (roll, pitch, yaw) will cause a change in the direction of quadcopter translational movement. So, the total forces of the quadcopter can be decomposed into force elements in each axis (F_x, F_y, F_z). Figure 3 shows the illustration of force decomposition to each axis in body frame {B}.

$$F_{total} = \sum_{i=1}^{4} F_i \quad (3)$$

Equation (4) is rotation matrix of quadcopter. C, S are cosine and sine function respectively.

$$R = \begin{bmatrix} C\phi C\theta & C\phi S\theta S\psi - C\psi S\phi & S\phi S\psi + C\phi C\psi S\theta \\ C\theta S\phi & C\phi C\psi + S\phi S\theta S\psi & C\psi S\phi C\theta - C\phi S\psi \\ -S\theta & C\theta S\psi & C\theta C\psi \end{bmatrix} \quad (4)$$

The derived model of quadcopter translational movement can be represented as equation (5). Where $\ddot{x}, \ddot{y}, \ddot{z}$ are linear acceleration in of quadcopter in each axis.

$$m\begin{bmatrix} \ddot{x} \\ \ddot{y} \\ \ddot{z} \end{bmatrix} = R\begin{bmatrix} 0 \\ 0 \\ F_{total} \end{bmatrix} - \begin{bmatrix} 0 \\ 0 \\ mg \end{bmatrix} \quad (5)$$

The model also contains a gyroscopic effect. Derived torque models of quadcopter are presented in equation (6), (7), and (8).

$$\tau_x = \begin{bmatrix} F_1 \\ F_2 \\ F_3 \\ F_4 \end{bmatrix}^T l \begin{bmatrix} C(\frac{\pi}{4}) \\ C(\frac{3\pi}{4}) \\ C(\frac{5\pi}{4}) \\ C(\frac{7\pi}{4}) \end{bmatrix} + \dot{\theta}\dot{\psi}(I_{yy} - I_{zz}) \quad (6)$$

$$\tau_y = \begin{bmatrix} F_1 \\ F_2 \\ F_3 \\ F_4 \end{bmatrix}^T l \begin{bmatrix} S(\frac{\pi}{4}) \\ S(\frac{3\pi}{4}) \\ S(\frac{5\pi}{4}) \\ S(\frac{7\pi}{4}) \end{bmatrix} + \dot{\phi}\dot{\psi}(I_{zz} - I_{xx}) \quad (7)$$

$$\tau_z = K_d l(-F_1 + F_2 - F_3 + F_4) + \dot{\theta}\dot{\phi}(I_{xx} - I_{yy}) \quad (8)$$

τ_x, τ_y, τ_z are roll, pitch, and yaw torque respectively. l is distance of rotor between center of mass. $\dot{\phi}, \dot{\theta}, \dot{\psi}$ are roll, pitch, and yaw angular body speed respectively. I_{xx}, I_{yy}, I_{zz} are roll, pitch, and yaw body inertia respectively. K_d is force resistance constant in equation (2).

Let us define the control inputs of quadcopter are u_1, u_2, u_3, u_4. Where u_1 is total force to control input. Total force control input can be

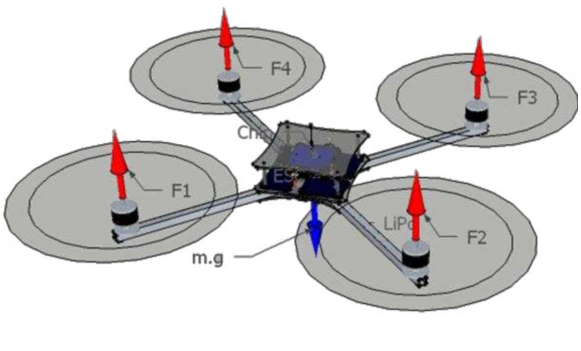

Figure 2. Force distribution in quadcopter

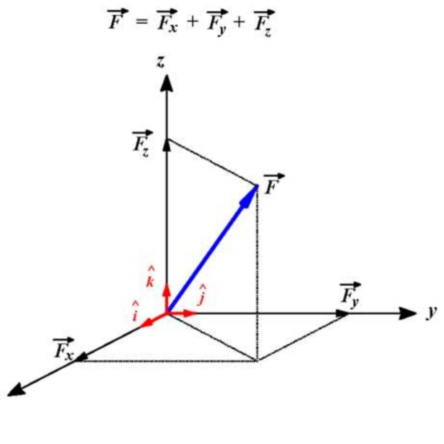

Figure 3. Total forces illustration that decomposed into each axis

derived by substituting equation (1) to (3). u_2 is roll torque control input, u_3 is pitch torque control input, and u_4 is yaw torque control input can be derived by substituting equation (1) to (6)-(7) and equation (2) to (8). Where, k_t and k_d are constant values from equation (1) and (2).

$$\begin{aligned} u_1 &= F_{total} \\ &= k_t \sum_{i=1}^{4} \Omega_i^2 \\ u_2 &= \tau_x \\ &= k_t l \sum_{i=1}^{4} \Omega_i^2 \cos(\tfrac{\pi}{2}(i-1) + \tfrac{\pi}{4}) \\ u_3 &= \tau_y \\ &= k_t l \sum_{i=1}^{4} \Omega_i^2 \sin(\frac{\pi}{2}(i-1) + \frac{\pi}{4}) \\ u_4 &= \tau_z \\ &= k_d l \sum_{i=1}^{4} (-1)^i \Omega_i^2 \end{aligned} \tag{9}$$

By substituting equation (9) into (5) to (8), the derived model of quadcopter in (10).

$$\begin{aligned} \ddot{x} &= \frac{(S\phi S\psi + C\phi C\psi S\theta)u_1}{m} \\ \ddot{y} &= \frac{(C\psi S\phi C\theta - C\phi S\psi)u_1}{m} \\ \ddot{z} &= \frac{(C\theta S\psi)u_1}{m} - g \\ \ddot{\phi} &= \frac{u_2 + \dot{\theta}\dot{\psi}(I_{yy} - I_{zz})}{I_{xx}} \\ \ddot{\theta} &= \frac{u_3 + \dot{\phi}\dot{\psi}(I_{zz} - I_{xx})}{I_{yy}} \\ \ddot{\psi} &= \frac{u_4 + \dot{\theta}\dot{\phi}(I_{xx} - I_{yy})}{I_{zz}} \end{aligned} \tag{10}$$

where $\ddot{\phi}, \ddot{\theta}, \ddot{\psi}$ are roll, pitch, yaw, angular acceleration at quadcopter body.

III. QUADCOPTER CONTROLLER DESIGN

In this section, the control algorithm of quadcopter is presented. The purpose is to combine PD and AFC as rotational controller to stabilize quadcopter. Figure 4 shows quadcopter control structure. Figure 5 shows the proposed rotational controller to stabilize quadcopter. In this simulation, translational movement are neglected. The controller design is focused to stabilize the quadcopter toward disturbance. PD controller is used to stabilize quadcopter and AFC to reject uncertainty disturbance from environment. In this simulation, quadcopter get constant and fluctuated disturbance.

From Figure 4, the relationship of each input and each state can be represented as:

$$\begin{aligned} \dot{X} &= AX + BU \\ X &= [\phi \quad \theta \quad \psi \quad \dot{\phi} \quad \dot{\theta} \quad \dot{\psi}]^T \\ U &= [u_1 \quad u_2 \quad u_3 \quad u_4]^T \\ \dot{X} &= [\dot{\phi} \quad \dot{\theta} \quad \dot{\psi} \quad \ddot{\phi} \quad \ddot{\theta} \quad \ddot{\psi}]^T \end{aligned} \tag{11}$$

The system matrix (A) can be represented as:

$$A = \begin{bmatrix} 0 & 0 & 0 & 1 & 0 & 0 \\ 0 & 0 & 0 & 0 & 1 & 0 \\ 0 & 0 & 0 & 0 & 0 & 1 \\ 0 & 0 & 0 & 0 & \frac{\dot{\psi}(I_{yy}-I_{zz})}{2I_{xx}} & \frac{\dot{\theta}(I_{yy}-I_{zz})}{2I_{xx}} \\ 0 & 0 & 0 & \frac{\dot{\psi}(I_{zz}-I_{xx})}{2I_{yy}} & 0 & \frac{\dot{\phi}(I_{zz}-I_{xx})}{2I_{yy}} \\ 0 & 0 & 0 & \frac{\dot{\theta}(I_{xx}-I_{yy})}{2I_{zz}} & \frac{\dot{\phi}(I_{xx}-I_{yy})}{2I_{zz}} & 0 \end{bmatrix} \tag{12}$$

The control matrix (B) can be represented as:

$$B = \begin{bmatrix} 0 & 0 & 0 & 0 \\ 0 & 0 & 0 & 0 \\ 0 & 0 & 0 & 0 \\ 0 & \frac{1}{I_{xx}} & 0 & 0 \\ 0 & 0 & \frac{1}{I_{yy}} & 0 \\ 0 & 0 & 0 & \frac{1}{I_{zz}} \end{bmatrix} \tag{13}$$

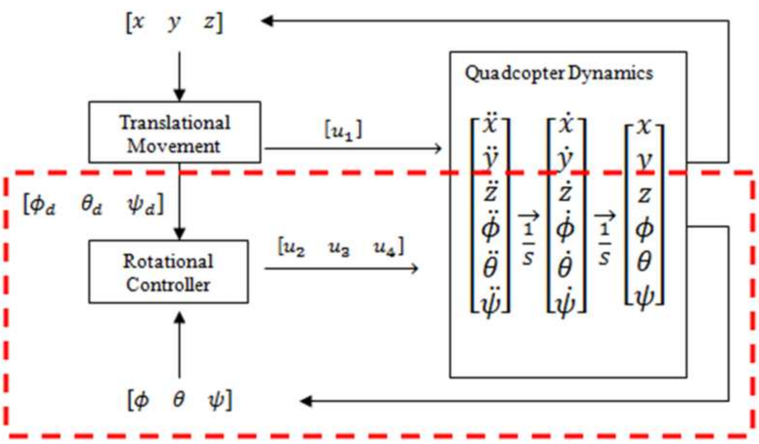

Figure 4. Quadcopter control structure

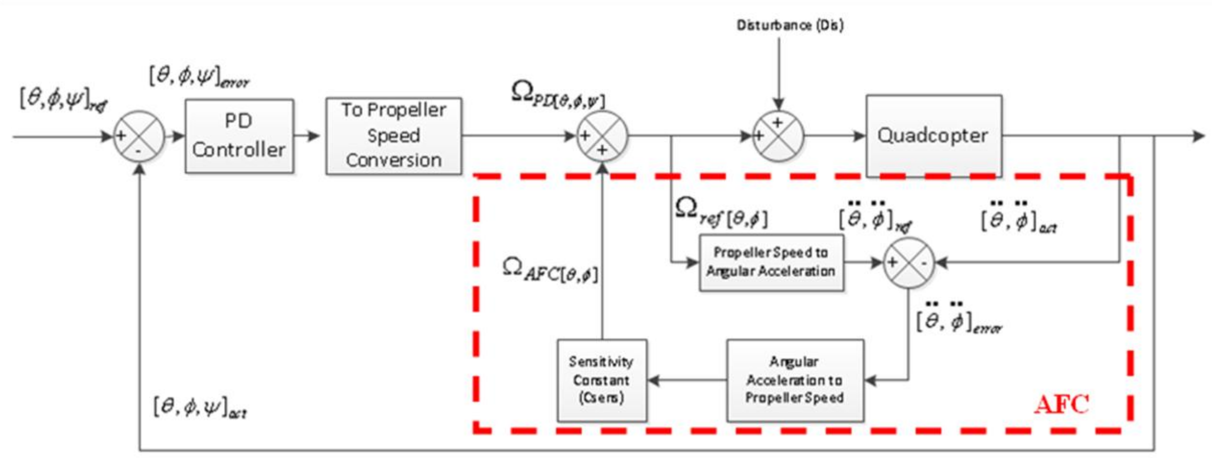

Figure 5. The proposed rotational controller

A. Disturbance Model

In this subsection, the model of disturbance will be presented. Figure 1 shows disturbance position of quadcopter, disturbance mass located at (L_{DXB}, L_{DYB}) from the center of quadcopter in (XB, YB) axis. State equation (11) can be written as follows:

$$\dot{X} = AX + BU + Dis \tag{14}$$

The simulation disturbance is:

$$Dis = [0 \quad 0 \quad 0 \quad Dis_X.L_{DYB} \quad Dis_X.L_{DXB} \quad 0]^T \tag{15}$$

B. PD Controller Design

PD controller will be presented to stabilize quadcopter. The reason is this controller very simple and easy implemented. In this section, PD control algorithm is designed without disturbance parameter. The controller design is focused to stabilize quadcopter when hovering without get uncertainty disturbance. The model that presented at section 2 is completed by gyroscopic effect. Gyroscopic effect can be ignored because it does not have significant effect on quadcopter system [14]. The model can be simplified:

$$\ddot{\phi} = \frac{k_t l \sum_{i=1}^{4} \omega_i^2 \cos(\frac{\pi}{2}(i-1)+\frac{\pi}{4})}{I_{xx}}$$
$$\ddot{\theta} = \frac{k_t l \sum_{i=1}^{4} \omega_i^2 \sin(\frac{\pi}{2}(i-1)+\frac{\pi}{4})}{I_{yy}} \tag{16}$$
$$\ddot{\psi} = \frac{k_d l \sum_{i=1}^{4} (-1)^i \omega_i^2}{I_{zz}}$$

The simulation purposes to stabilize roll, pitch, and yaw angle. Integrating twice about time and introducing s operator in equation (16), the model can be rewritten as:

$$\phi = \frac{k_t l \sum_{i=1}^{4} \omega_i^2 \cos(\frac{\pi}{2}(i-1)+\frac{\pi}{4})}{I_{xx}s^2}$$
$$\theta = \frac{k_t l \sum_{i=1}^{4} \omega_i^2 \sin(\frac{\pi}{2}(i-1)+\frac{\pi}{4})}{I_{yy}s^2} \tag{17}$$
$$\psi = \frac{k_d l \sum_{i=1}^{4} (-1)^i \omega_i^2}{I_{zz}s^2}$$

From equation (17), the model is second order form, in order to make it possible to design multiple PD controllers for this system, one can neglect gyroscopic effects and thus remove the cross coupling [1]. This is PD controller for each orientation angle.

$$u_2, u_3, u_4 = P_{\phi,\theta,\psi}(\phi,\theta,\psi) + D_{\phi,\theta,\psi}(\phi,\theta,\psi) \tag{18}$$

where u_2, u_3, u_4 are control input for roll, pitch, yaw torque respectively; $P_{\phi,\theta,\psi}(\phi,\theta,\psi)$ are proportional control for roll, pitch, and yaw respectively; $D_{\phi,\theta,\psi}(\phi,\theta,\psi)$ are derivative control for roll, pitch, and yaw respectively.

C. AFC Controller Design

AFC controller is designed to reject uncertainty disturbance from environment. Figure 6 shows AFC block diagram that used in simulation. This block has two inputs, they are measured angular velocity and applied propeller speed.

Let us define γ as rotation angle roll and pitch axis (ϕ, θ),

$$\ddot{\gamma} = \frac{d\dot{\gamma}}{dt} \tag{19}$$

$$\Omega_\phi = \Omega_1 + \Omega_2 - \Omega_3 - \Omega_4$$
$$\Omega_\theta = \Omega_1 - \Omega_2 - \Omega_3 + \Omega_4 \tag{20}$$

$$\ddot{\gamma}_{ref} = \frac{0.5\rho C_T l \Omega_\gamma |\Omega_\gamma|}{I_{xx,yy}} \tag{21}$$

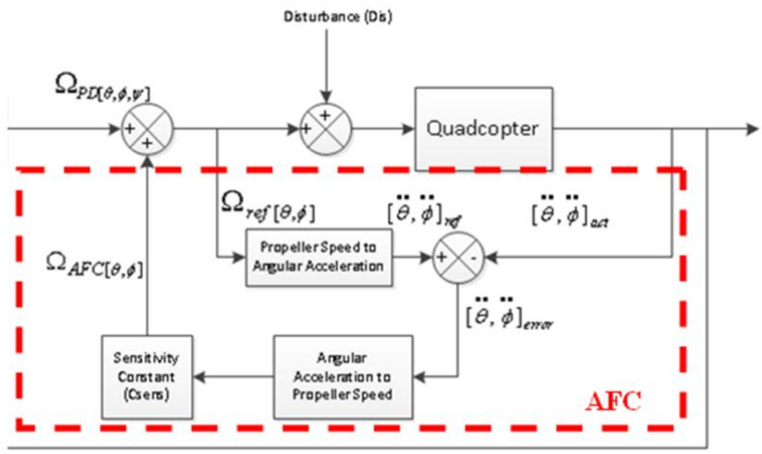

Figure 6. AFC block diagram

$$\ddot{\gamma}_{AFC} = \ddot{\gamma}_{ref} - \ddot{\gamma} \quad (22)$$

$$\Omega_{AFC} = C_{sens}\left(\frac{\ddot{\gamma}_{AFC} I_{xx,yy}}{0.5\rho C_T l}\right)^{0.5}, \quad \text{with } 0 \leq \ddot{\gamma}_{AFC} \leq 1$$
$$= K_{AFC}\left(\ddot{\gamma}_{ref} - \ddot{\gamma}\right) \quad (23)$$

First input is measured angular velocity that differentiated into actual angular acceleration in equation (19). Second input is applied propeller speed that converted into angular acceleration reference in equation (21). $\ddot{\gamma}_{AFC}$ is estimated disturbance acceleration. To get estimated disturbance, actual angular acceleration is compared by angular acceleration reference in equation (22) [11]. Last, convert the disturbance acceleration into propeller speed in equation (23) then add the result with PD controller result. C_{sens} is a constant value to set AFC sensitivity output toward disturbance, then simplified to K_{AFC}. Ω_{AFC} is propeller speed calculation of AFC controller output.

IV. Simulation Result

The simulation test was performed using SIMULINK to evaluate the performance of the controller. The simulation model (10) was used in S-Function block. In this simulation, the model contain disturbance that has been modeled in section 3, there are constant and fluctuated disturbances.

Before doing some simulation process, the parameters of quadcopter must be collected from real data. This simulation used quadcopter data obtained from [16]. They are listed in Table 1.

PD coefficients that used for simulations were derived by trial and error to get best performance, the PD parameter are listed in Table 2. First simulation compared PD and PDAFC performance when they constant disturbance. Second, third, and fourth simulation compared PD and PDAFC performance when they fluctuate disturbance using sinusoid disturbance, sawtooth disturbance, and pulse disturbance. Then, Root Mean Square (RMS) method was used to determine the controller performance analysis. Lower RMS error value means better performance of controller. Figure 7 shows the simulation result of PD method and PDAFC method with constant disturbance. In this simulation, PDAFC was tested with three

Table 1.
Quadcopter simulation parameter

Parameter	Unit	Value
M	kg	1.025
L	meter	0.270
k_t	Ns^2	3.122e-06
k_d	Nms^2	1.759e-08
Ixx,Iyy	kgm^2	0.012
Izz	kgm^2	0.048
Dis_X	N	Amp x Waveform(Freq) 1. 0.2 2. 0.2 x S (2π0.4t) 3. 0.2 x sawtooth (0.4 Hz) 4. 0.2 x square (0.4 Hz)
L_{DXB}	mm	0
L_{DYB}	mm	190

Table 2.
PD coefficients simulation parameter

Parameter	Value
KP roll	0.097
KD roll	0.036
KP pitch	0.097
KD pitch	0.036
KP yaw	0.0001368
KD yaw	0.0000684

sensitivities constants (C_{sens}) in equation (23), they were 0.13, 0.15 and 0.18. By using PD, maximum error is 0.326 radian with RMS valued is 0.060. PDAFC with 0.13 constant, maximum error is 0.153 radian and RMS value is 0.029. Then with 0.15 constant, maximum error is 0.125 radian and RMS value is 0.017, it can stable in 5 seconds. Last is PDAFC with 0.18 constant, maximum error is 0.090 radian and RMS value is 0.018, but still noisy because of the controller became more sensitive with disturbance.

Figure 8 shows second simulation result to compare PD method and PDAFC method with sine function disturbance. In this simulation, disturbance maximum amplitude was 0.2 with frequency 0.4 Hz. PDAFC was tested with three sensitivities constant (C_{sens}) in equation (23), which were 0.13, 0.15 and 0.18. PD maximum error is 0.394 radian with RMS value of 0.255. PDAFC with 0.13 constant, maximum error was 0.210 radian and RMS value is 0.121. Then with 0.15 constant, maximum error is 0.161 radian and RMS value is 0.098. Last is PDAFC with 0.18 constant, maximum error is 0.130 radian and RMS value is 0.074. PDAFC with 0.18 constant give lowest RMS error value.

Figure 9 shows third simulation by using sawtooth function disturbance. In this simulation, disturbance maximum amplitude is 0.2 with frequency 0.4 Hz. PDAFC was tested with three sensitivities constant (C_{sens}), they were 0.13, 0.15 and 0.18. PD maximum error is 0.241 radian with RMS valued is 0.186. PDAFC with 0.13 constant, maximum error is 0.241 radian and RMS value is 0.092. Then with 0.15 constant, maximum error is 0.199 radian and RMS value is 0.073. Last is PDAFC with 0.18 constant, maximum error is 0.156 radian and RMS value is 0.055. PDAFC with 0.18 constant give lowest RMS error value.

Figure 10 shows fourth simulation by using square function disturbance. In this simulation, disturbance maximum amplitude was 0.2 with frequency 0.4 Hz. PDAFC was tested with three sensitivities constant (C_{sens}), they were 0.13, 0.15 and 0.18. PD maximum error is 0.575 radian, RMS value is 0.317. PDAFC with 0.13 constant, maximum error is 0.315 radian and

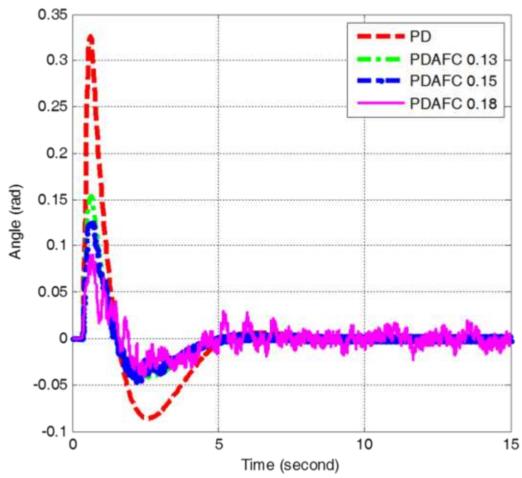

Figure 7. Constant disturbance simulation result

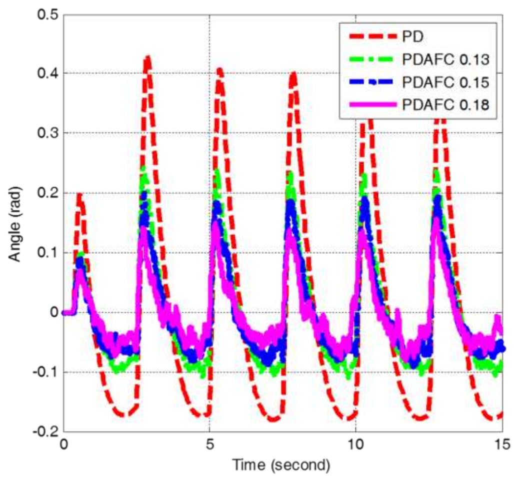

Figure 9. Sawtooth disturbance simulation result

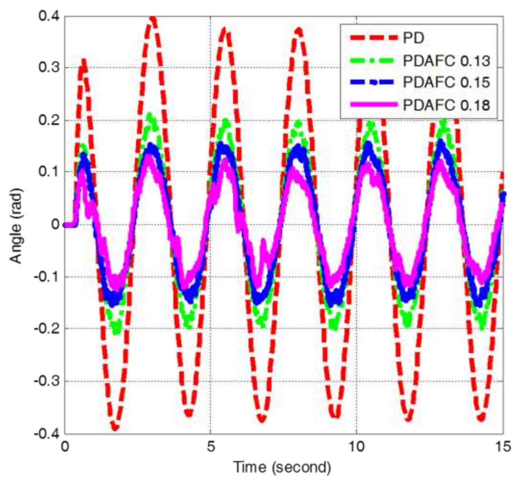

Figure 8. Sine disturbance simulation result

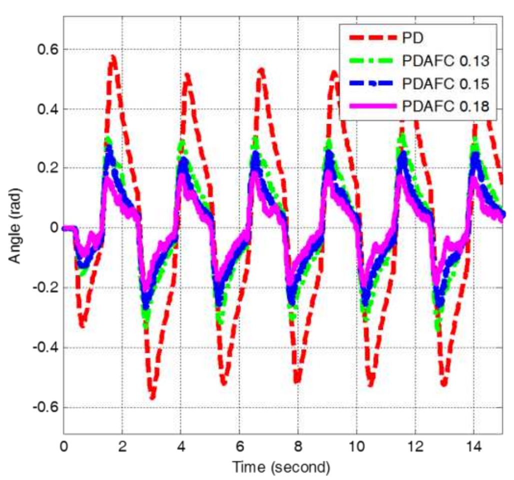

Figure 10. Square disturbance pulse simulation result

RMS value is 0.170. Then with 0.15 constant, maximum error is 0.272 radian and RMS value is 0.128. Last is PDAFC with 0.18 constant, maximum error is 0.190 radian and RMS value is 0.092. PDAFC with 0.18 constant give lowest RMS error value.

V. CONCLUSION

An “x” configuration quadcopter has been successfully modeled. Then, simulation results have been presented to show the controller performance. By adding PD with AFC, better result was obtained. From the simulation, PDAFC controller can minimize the effect of disturbance. Inconstant disturbance simulation, the best sensitivity constant (C_{sens}) was obtained when the value was 0.15, the quadcopter maximum error 0.125 radian and could stable in 5 seconds. In fluctuated simulation result, PDAFC with 0.18 constant gave lowest RMS error value, 0.074 radian for sine disturbance, 0.055 radian for sawtooth disturbance, and 0.092 radian for square pulse disturbance.

ACKNOWLEDGEMENT

The author would like to thank the Electronic Engineering Polytechnic Institute of Surabaya for giving laboratories facilities for the research.

REFERENCES

[1] Bouabdallah et al. "PID vs LQ control techniques applied to an indoor micro quadrotor." *Intelligent Robots and Systems, 2004.(IROS 2004). Proceedings. 2004 IEEE/RSJ International Conference on*. Vol. 3. IEEE, 2004, pp.2451-2456.

[2] Li, Jun, and Yuntang Li. "Dynamic analysis and PID control for a quadrotor."*Mechatronics and Automation (ICMA), 2011 International Conference on*. IEEE, 2011, pp. 573-578.

[3] Mokhtari et al. "Dynamic feedback controller of Euler angles and wind parameters estimation for a quadrotor unmanned aerial vehicle." *Robotics and Automation, 2004. Proceedings. ICRA'04. 2004 IEEE International Conference on*. Vol. 3. IEEE, 2004, pp. 2359-2366.

[4] Gupte et al. "A survey of quadrotor Unmanned Aerial Vehicles." *Southeastcon, 2012 Proceedings of IEEE*. IEEE, 2012, pp. 1-6.

[5] Erginer et al."Modeling and PD control of a quadrotor VTOL vehicle." *Intelligent Vehicles Symposium, 2007 IEEE*. IEEE, 2007, pp. 894-899.

[6] Pounds et al."Modelling and control of a large quadrotor robot." *Control Engineering Practice* 18.7 Elsevier, pp. 691-699, 2010.

[7] Tayebi, A., and S. McGilvray. "Attitude stabilization of a four-rotor aerial robot." *Decision and Control, 2004. CDC. 43rd IEEE Conference on*. Vol. 2. IEEE, 2004, pp. 1216-1221.

[8] Sumantri et al. "Robust tracking control of a quad-rotor helicopter utilizing sliding mode control with a nonlinear sliding surface." *Journal of System Design and Dynamics* 7, no. 2, pp. 226-241, 2013.

[9] Ming Chen and MihaiHuzmezan, “A combined MBPC/2DOF H∞ controller for a quadrotor UAV”, Proceeding of AIAA guidance, navigation, and control conference and exhibit, Texas- USA, 11-14 August 2003.

[10] Estiko Rijanto, “*Robust control: theory for application*”, ISBN: 979-9299-12-8, Bandung: ITB Press, 2000.

[11] Pitowarno, Endra. "An implementation of a knowledge-based system method to an active force control robotic scheme." *Master Thesis, Universiti Teknologi Malaysia,* 2002.

[12] Katsura, Seiichiro et al. "Modeling of force sensing and validation of disturbance observer for force control." *Industrial Electronics, IEEE Transactions on* 54, no. 1, pp. 530-538, 2007.

[13] Chen, Wen-Hua. "Disturbance observer based control for nonlinear systems." *Mechatronics, IEEE/ASME Transactions on* 9, no. 4, pp. 706-710, 2004.

[14] Bouabdallah et al."Design and control of an indoor micro quadrotor." *Robotics and Automation, 2004. Proceedings. ICRA'04. 2004 IEEE International Conference on*. Vol. 5. IEEE, 2004, pp. 4393-4398.

[15] Benallegue, A. et al. "Feedback linearization and high order sliding mode observer for a quadrotor UAV." *Variable Structure Systems, 2006. VSS'06. International Workshop on*. IEEE, 2006, pp. 365-372.

[16] Ni’am Tamami et al."Modelling and PD control for “x” configuration quadcopter." *Indonesian Symposium on Robot Soccer Competition, 2013. Proceedings.* Dian Nuswantoro University. ISBN:979-26-0264-X, Semarang: Dian Nuswantoro University Press, 2013, pp. 98-103.